41st Annual International Conference of the IEEE Engineering in Medicine and Biology Society

July 23-27 2019

Messe Berlin
Berlin, Germany

Conference Chair

Thomas Penzel, Charité University Medicine Berlin, Germany

Conference Co-Chairs

Thomas Lenarz, Medical University of Hannover (MHH), Germany

Mohamad Sawan, Westlake University Hangzhou, China

Program Chair

Olaf Dössel, Karlsruhe Institute of Technology, Germany

Program Co-Chairs

Luca Mainardi, Politecnico di Milano, Italy
Konstantina S. Nikita, National Technical University of Athens, Greece
James Weiland, University of Michigan Ann Arbor, United States

IEEE Advancing Technology for Humanity

EMB

Indexed in PubMed® and MEDLINE®, Products of the United States National Library of Medicine

PubMed MEDLINE U.S. National Library of Medicine

Table of Contents

14:15-14:30 SaC03.6
Ultrasound-Based Regularized Log Spectral Difference Method for Monitoring Microwave Hyperthermia
Kothawala, AliArshad *(Indian Institute of Technology Madras)*; Baskaran, Divya Baskaran *(Indian Institute of Technology Madras)*; Arunachalam, Kavitha *(Duke University)*; Thittai, Arun Kumar* *(IIT MADRAS)*

SaC04: 13:00-14:30 Hall A1 – Level 1
Biomechanical Analysis (Oral Session)
Chair: Cereatti, Andrea *(University of Sassari)*
Co-Chair: Doheny, Emer *(University College Dublin)*

13:00-13:15 SaC04.1
Synthesising Motion Sensor Data from Biomechanical Simulations to Investigate Motion Sensor Placement and Orientation Variations
Derungs, Adrian* *(Friedrich-Alexander-Universität Erlangen-Nürnberg (FAU))*; Amft, Oliver *(Friedrich-Alexander Universität Erlangen-Nürnberg (FAU))*

13:15-13:30 SaC04.2
IMU-Based Assessment of Ankle Inversion Kinematics and Orthosis Migration
Betz, Johannes *(TU Berlin)*; Klingspor, Christoph *(TU Berlin)*; Seel, Thomas* *(Technische Universität Berlin)*

13:30-13:45 SaC04.3
Three-Dimensional GRF and CoP Estimation during Stair and Slope Ascent/Descent with Wearable IMUs and Foot Pressure Sensors
Fukushi, Kenichiro* *(NEC Corporation)*; Sekiguchi, Yusuke *(Tohoku Univ.)*; Honda, Keita *(Tohoku Univ.)*; Yaguchi, Haruki *(Tohoku Univ.)*; Izumi, Shin-ichi *(Tohoku Univ.)*

13:45-14:00 SaC04.4
Hand Motion Measurement using Inertial Sensor System and Accurate Improvement by Extended Kalman Filter
Kitano, Keisuke* *(Doshisha University)*; Ito, Akihito *(Doshisha University)*; Tsujiuchi, Nobutaka *(Doshisha University)*

14:00-14:15 SaC04.5
Regression-Based Analysis of Front Crawl Swimming using Upper-Arm Mounted Accelerometers
Doheny, Emer* *(Univ. College Dublin)*; Goulding, Cathy *(Univ. College Dublin)*; Lowery, Madeleine *(Univ. College Dublin)*

14:15-14:30 SaC04.6
Inter-Leg Distance Measurement as a Tool for Accurate Step Counting in Patients with Multiple Sclerosis
Bertuletti, Stefano* *(University of Sassari)*; Salis, Francesca *(University of Sassari)*; Cereatti, Andrea *(University of Sassari)*; Angelini, Lorenza *(University of Sheffield)*; Buckley, Ellen *(University of Sheffield)*; Nair, K.P.S. *(Sheffield Teaching Hospitals NHS Foundation Trust)*; Mazzà, Claudia *(University of Sheffield)*; Della Croce, Ugo *(University of Sassari)*

SaC05: 13:00-14:30 Hall A2 – Level 1
Connectivity and Causality (Oral Session)
Chair: Astolfi, Laura *(University of Rome Sapienza)*

13:00-13:15 SaC05.1
Recurrent Neural Networks for Reconstructing Complex Directed Brain Connectivity
Duggento, Andrea* *(University of Rome "Tor Vergata")*; Guerrisi, Maria *(University of Rome "Tor Vergata")*; Toschi, Nicola *(University of Rome "Tor Vergata", Faculty of Medicine)*

13:15-13:30 SaC05.2
Single-Trial Connectivity Estimation through the Least Absolute Shrinkage and Selection Operator
Antonacci, Yuri* *(University of Rome Sapienza)*; Toppi, Jlenia *(University of Rome "Sapienza")*; Mattia, Donatella *(Fondazione Santa Lucia IRCCS)*; Pietrabissa, Antonio *(University of Rome Sapienza)*; Astolfi, Laura *(University of Rome Sapienza)*

13:30-13:45 SaC05.3
Effect of Connectivity Measures on the Identification of Brain Functional Core Network at Rest
Rizkallah, Jennifer* *(LTSI Inserm U1099, Univ. de Rennes 1)*; Amoud, Hassan *(Lebanese Univ.)*; Wendling, Fabrice *(INSERM – Univ. de Rennes 1)*; Hassan, Mahmoud *(Univ. de Rennes 1)*

13:45-14:00 SaC05.4
Tracking Changes in Brain Network Connectivity under Transcranial Current Stimulation
Jami, Apoorva Sargarwal *(New York Univ.)*; Guo, Xinling *(Zhejiang Univ.)*; Kulkarni, Prathamesh *(Univ. of Houston)*; Henin, Simon *(NYU School of Medicine)*; Liu, Anli *(New York Univ. Langone Health)*; Chen, Zhe* *(New York Univ. School of Medicine)*

14:00-14:15 SaC05.5
Analysis of Volume Conduction Effects on Different Functional Connectivity Metrics: Application to Alzheimer's Disease EEG Signals
Ruiz-Gómez, Saúl J. *(Biomedical Engineering Group, Univ. of Valladolid)*; Gomez, Carlos* *(Univ. of Valladolid)*; Poza, Jesus *(Univ. of Valladolid)*; Maturana-Candelas, Aarón *(Univ. of Valladolid)*; Rodríguez-González, Víctor *(Biomedical Engineering Group, Univ. of Valladolid)*; Garcia, Maria *(Univ. of Valladolid)*; Tola-Arribas, Miguel A. *(Dept. of Neurology, Hospital Universitario Río Hortega)*; Cano, Mónica *(Dept. of Clinical Neurophysiology, Hospital Universitario R)*; Hornero, Roberto *(Univ. of Valladolid)*

14:15-14:30 SaC05.6
Time-Varying Effective EEG Source Connectivity: The Optimization of Model Parameters
Rubega, Maria* *(Univ. of Geneva)*; Pascucci, David *(Univ. of Fribourg)*; Rué Queralt, Joan *(Dept. of Radiology, Lausanne Univ. Hospital & Univer)*; van Mierlo, Pieter *(Ghent Univ., Epilog NV)*; Hagmann, Patric *(Dept. of Radiology, Univ. Hospital Center (CHUV) & U)*; Plomp, Gijs *(Univ. of Fribourg)*; Michel, Christoph *(Univ. of Geneva)*

SaC06: 13:00-14:30 Hall A5 – Level 1
Neural Stimulation (III) (Oral Session)

13:00-13:15 SaC06.1
High-Resolution Head Model of Transcranial Direct Current Stimulation: A Labeling Analysis
Thomas, Chris *(Soterix Medical, Inc.)*; Huang, Yu *(City College of New York)*; Faria, Paula Cristina *(ESTG, CDRSP, IPLeiria)*; Datta, Abhishek* *(Soterix Medical, Inc.)*

13:15-13:30 SaC06.2
Cortical Stimulation Induces Network-Wide Coherence Change in Non-Human Primate Somatosensory Cortex
Bloch, Julien *(Univ. of Washington, Seattle)*; Khateeb, Karam *(Univ. of Washington)*; Silversmith, Daniel *(Univ. of California, San Francisco)*; O'Doherty, Joseph E. *(Univ. of California, San Francisco)*; Sabes, Philip N. *(Univ. of California, San Francisco)*; Yazdan-Shahmorad, Azadeh* *(Univ. of Washington)*

13:30-13:45 SaC06.3
Quantification of Neural Conduction Block on the Rat Sciatic Nerve based on EMG Response
Pérez, Diego *(Univ. Rennes, CHU Rennes, Inserm, LTSI UMR 1099, Rennes)*; Dieuset, Gabriel *(LTSI, Inserm UMR 1099, Rennes, France; University Rennes 1, Fran)*; Yochum, Maxime *(Université de Rennes 1)*; Senhadji, Lotfi *(Université de Rennes 1 & INSERM)*; Martin, Benoit *(INSERM; Université de Rennes 1; LTSI)*; Le Rolle, Virginie *(University of Rennes 1)*; Hernández, Alfredo I* *(Univ. of Rennes 1 & INSERM U1099)*

13:45-14:00 SaC06.4
Learning State-Dependent Neural Modulation Policies with Bayesian Optimization
Connolly, Mark* *(Emory University)*; Park, Sang-Eon *(Georgia Institute of Technology)*; Gross, Robert *(Emory University)*

14:00-14:15 SaC06.5
Referred Sensation Areas in Transpelvic Amputee
Lontis, Eugen Romulus* *(Aalborg University)*; Yoshida, Ken *(Indiana University-Purdue University Indianapolis)*; Jensen, Winnie *(Center for Sensory-Motor Interaction)*

Analysis of Volume Conduction Effects on Different Functional Connectivity Metrics: Application to Alzheimer's Disease EEG Signals

Saúl J. Ruiz-Gómez, Carlos Gómez, *IEEE Senior Member*, Jesús Poza, *IEEE Senior Member*, Aarón Maturana-Candelas, Víctor Rodríguez-González, María García, *IEEE Senior Member*, Miguel Á. Tola-Arribas, Mónica Cano, Roberto Hornero, *IEEE Senior Member*

***Abstract*— The aim of this study was to evaluate the effect of volume conduction on different connectivity metrics: Amplitude Envelope Correlation (*AEC*), Phase Lag Index (*PLI*), and Magnitude Squared Coherence (*MSCOH*). These measures were applied to: (i) a synthetic model of 64 coupled oscillators; and (ii) a resting-state EEG database of 72 patients with dementia due to Alzheimer's disease (AD) and 37 cognitively healthy controls. Our results revealed that *AEC* and *PLI* are weakly influenced by the simulated volume conduction compared to *MSCOH*, although the three metrics are not immune to this effect. Furthermore, results with real EEG recordings showed that AD patients are characterized by an *AEC* increase in δ frequency band and widespread connectivity decreases in α and β_1 bands. These coupling changes reflect the abnormalities in spontaneous EEG activity of AD patients and might provide further insights into the underlying brain dynamics associated with this disorder.**

I. INTRODUCTION

The human brain can be seen as an extremely complex network governed by the interactions among billions of neurons [1]. Electroencephalography (EEG) measures the brain electrical activity generated by synchronized cortical neurons in a non-invasive way with a high temporal resolution. However, the main limitation of EEG is that there is no unique relation between the time series recorded from the scalp and the active neuronal sources in the brain [2]. Time series that are recorded from nearby sensors are very likely to pick up activity from the same brain sources, which gives rise to spurious correlations between them. This is known as the problem of 'volume conduction' [2].

Dementia due to Alzheimer's disease (AD) is a neurodegenerative disorder associated with cognitive, behavioral, and functional deficits. Neural activity from AD patients is progressively modified as a consequence of the pathophysiological processes [1]. For the EEG analysis in AD, local activation techniques in individual sensors (both spectral and non-lineal analyses) are the most extended option, due to their ease of clinical interpretation and simplicity [3]. However, it has become clear that simple activation studies are no longer sufficient for AD characterization [4]. In this regard, the application of connectivity metrics can be used to gain further understanding on how the AD brain is organized as a network. However, it is important to minimize the spurious correlations that can appear due to volume conduction [4]. Several models of synthetic signals have been applied with the aim of studying and characterizing the influence of volume conduction. In this study, we used the well-studied model of globally coupled limit-cycle oscillators that was originally described by Kuramoto [5]. This model allowed us to evaluate the ability of diverse connectivity metrics to detect real changes in synchronization.

Our main objective was to analyze how different connectivity metrics are affected by volume conduction. Specifically, the following research questions were addressed: (i) which of the analyzed connectivity metrics is able to detect real changes in synchronization without being affected by volume conduction?; and (ii) are these measures capable of reflecting brain alterations suffered by AD patients?

II. MATERIALS

A. Subjects

EEG resting-state activity was analyzed in 72 mild and moderate AD patients (age 81.8 [76.0 83.5] years, median [interquartile range]) and 37 cognitively healthy controls (age 75.8 [73.9 78.6] years). Patients with dementia due to AD were diagnosed according to the criteria of the National Institute on Aging and Alzheimer's Association (NIA-AA). The control group was composed of elderly subjects with no history of neurological or psychiatric disorders.

Participants and caregivers were informed about the research background and the study protocol. Moreover, all of them gave their written informed consent to be included in the study. The Ethical Committee of the 'Río Hortega' University Hospital (Valladolid, Spain) approved the study according to the Code of Ethics of the World Medical Association (Declaration of Helsinki).

This research was supported by 'European Commission' and 'European Regional Development Fund' (FEDER) under project 'Análisis y correlación entre el genoma completo y la actividad cerebral para la ayuda en el diagnóstico de la enfermedad de Alzheimer' ('Cooperation Programme Interreg V-A Spain-Portugal, POCTEP 2014-2020'), and by 'Ministerio de Ciencia, Innovación y Universidades' and FEDER under project DPI2017-84280-R. Saúl J. Ruiz-Gómez was in receipt of a predoctoral scholarship from the 'Junta de Castilla y León' and the 'European Social Fund'. Víctor Rodríguez-González was in receipt of a PIF-UVa grant from the University of Valladolid.

Saúl J. Ruiz-Gómez, Carlos Gómez, Jesús Poza, Aarón Maturana-Candelas, Víctor Rodríguez-González, María García, and Roberto Hornero are with the Biomedical Engineering Group, University of Valladolid, Valladolid, Spain (corresponding author's e-mail: saul.ruiz@gib.tel.uva.es).

Miguel Á. Tola-Arribas is with the Department of Neurology, 'Río Hortega' University Hospital, Valladolid, Spain.

Mónica Cano is with the Department of Clinical Neurophysiology, 'Río Hortega' University Hospital, Valladolid, Spain.

978-1-5386-1311-5/19/$31.00 ©2019 IEEE

B. Electroencephalographic recordings

EEG activity was recorded with a 19-channel system following the 10-20 International System (XLTEK®, Natus Medical). Five minutes of resting-state EEG activity were recorded at a sampling frequency of 200 Hz from the following electrodes: Fp1, Fp2, Fz, F3, F4, F7, F8, Cz, C3, C4, T3, T4, T5, T6, Pz, P3, P4, O1, and O2. Subjects were asked to remain with their eyes closed, still and awake during EEG acquisition.

Recordings were then preprocessed in three steps: (i) preliminary independent component analysis to remove components with artifacts; (ii) Hamming window FIR filtering to limit spectral content to the frequency band of [1 70] Hz; and (iii) visual selection of artifact-free epochs of 5s.

III. METHODS

A. Kuramoto model and synthetic signals

In order to study the influence of volume conduction on the ability of the different metrics to detect real changes in synchronization, we used a model of globally coupled oscillators that was originally proposed by Kuramoto [5]. The model describes the phase dynamics of a large network of N globally coupled limit-cycle oscillators. The phase dynamics are given by the following differential equation [5]:

$$\frac{d\theta_i}{dt} = \omega_i + \frac{K}{N}\sum_{j-1}^{N}\sin(\omega_j - \omega_i), \tag{1}$$

where θ_i denotes the phase of the ith oscillator, which has the natural frequency ω_i, and K is the strength of the connections between them.

The natural frequencies ω_i are typically collected from a Lorentzian distribution centered around ω_0 and width γ [6]:

$$g(\omega) = \frac{\gamma}{\pi[\gamma^2 + (\omega - \omega_0)^2]}, \tag{2}$$

Thus, the phase evolution of each oscillator is determined by its natural frequency ω_i and the average influence of all other oscillators whose natural frequency was obtained from the same ω_0.

Kuramoto showed that the system is not synchronized when $K < K_{crit}$, while a single cluster of synchronized oscillators emerges for $K > K_{crit}$ [5]. As the natural frequencies are taken from a Lorentzian distribution, this critical value is given by $K_{crit} = 2\gamma$ [2].

For each oscillator, Eq. (1) was numerically integrated with a time step of 5 ms (corresponding to a sample frequency of 200 Hz, the same sample frequency of the real EEG recordings). In all simulations, the initial 10 s were discarded to eliminate transients. The state of oscillator i, which was obtained from ω_0, at time t is given by [5]:

$$O_{i,\omega_0}(t) = A_{\omega_0}\sin(\theta_i), \tag{3}$$

where A_{ω_0} was a constant amplitude equal across oscillators obtained with the same ω_0, but frequency-dependent. The resulting time series simulate the activity of the cerebral sources and are used to create the synthetic EEG signals.

The voltage $V_k(t)$ of the kth EEG channel was related to the state $O_j(t)$ of the jth oscillator at time t as [2]:

$$V_k(t) = \frac{1}{2i_0+1}\sum_{j=k-i_0}^{j=k+i_0}\sum^{\omega_0} O_{j,\omega_0}(t), \tag{4}$$

where i_0 represents the volume conduction contribution for each EEG channel. In accordance with real EEG recordings, a total of 19 EEG channels were simulated. Finally, the preprocessing procedure described for the real EEG recordings was also applied to these synthetic signals.

To simulate the model, we took the central frequency by evaluating the range $f_0 \in [1.5, 69.5]$ Hz (step=1), that was obtained from dividing the $1-70$ Hz spectrum into spectral bands of 1 Hz wide ($\omega_0 = 2\pi f_0$). We have simulated $N = 64$ globally coupled oscillators for each frequency band. Although theoretically an infinite number of oscillators is necessary for the analytical results to hold, it has been shown that with a limited number of oscillators the model can be readily used to explain various empirical results [7]. The oscillation frequency was determined with a central frequency of ω_0 and a width of the Lorentzian distribution of $\gamma = 1$, defined according to a previous study [2]. In order to determine the state of each oscillator, values of A_{ω_0} were determined as the square root of the relative power in each frequency band centered at ω_0 (obtained from real EEG recordings taking into account only healthy control subjects). Simulations were performed for the different combinations of $i_0 = [0, 2, 4]$ (where $i_0 = 0$ represents the ideal volume conduction-free case, while $i_0 = 2$ and $i_0 = 4$ simulate two scenarios increasingly affected by volume conduction), and $K \in [0, 4]$ in steps of 0.5 (where higher K values indicate higher coupling strength between oscillator and higher synchronization between synthetic signals from simulated electrodes). For each value of i_0 and K, 20 trials of 5 s were calculated, resulting synthetic time series of 19 channels and 1000 samples that were subjected to connectivity analyses.

B. Connectivity metrics

In order to characterize the connectivity between the synthetic and real EEG signals of different pairs of electrodes, three complementary coupling metrics were analyzed: Amplitude Envelope Correlation (AEC), Phase Lag Index (PLI), and Magnitude Squared Coherency ($MSCOH$).

AEC is an estimation of the correlation of the amplitudes of two time series. It is obtained by means of their power envelopes using the Hilbert transform. Then, coupling is calculated by computing the Pearson correlation between the log transformed power envelopes [8]. Time series were orthogonalized for each time-window separately before computing the AEC to remove spatial leakage effects [9].

PLI quantifies the asymmetry in the distribution of phase differences calculated from the instantaneous phases of two time-series [2]:

$$PLI = |\langle sign\sin(\Delta\phi)\rangle|, \tag{5}$$

where $\langle\cdot\rangle$ indicates the expectation operator and $\Delta\phi$ is the phase difference or relative phase.

$MSCOH$ combines sensitivity to both amplitude and phase synchrony, and is defined as [10]:

$$MSCOH_{X,Y}(f) = \frac{|S_{XY}|^2}{P_X P_Y}, \quad (6)$$

where S_{XY} is the cross-spectrum of X and Y, and P_X and P_Y are the power spectral density of X and Y, respectively.

C. Statistical analysis

Firstly, a descriptive analysis with the synthetic data was carried out to study how the connectivity metrics are affected by volume conduction with the Two-sample Kolmogorov-Smirnov test (ks statistic). The lower the values of the ks statistic, the lesser the differences between the curves. Then, the ability of these metrics to obtain statistical differences between groups with real EEG recordings were evaluated with the Mann-Whitney U-test.

IV. RESULTS

A. Kuramoto model

Results for the Kuramoto models as a function of the global intensity of coupling between the oscillators (K) and the different volume conduction contribution values (i_0) are summarized in Fig. 1. The solid lines indicate the average coupling values and the shaded areas represent the standard deviation of the 20 simulated epochs.

Firstly, in the ideal case without volume conduction ($i_0 = 0$), AEC showed low values for $K < K_{crit} = 2$, and increasing values as K increments. When volume conduction was introduced AEC became slightly higher, especially for $K > 2$. Quantitatively, test statistic ks showed low values (0.21 and 0.28) for both volume conduction scenarios ($i_0 = 2$ and $i_0 = 4$, respectively) compared to $i_0 = 0$. Secondly, PLI stayed relatively low for $K < K_{crit}$ in the case of $i_0 = 0$. However, an increasing trend in PLI values can be noticed starting at $K = 1$, rather than at the theoretic value of $K_{crit} = 2$. PLI also showed higher values in both volume conduction scenarios, but is slightly less affected to its spurious influence compared to AEC ($ks = 0.18$ for $i_0 = 2$ and $ks = 0.27$ for $i_0 = 4$). Finally, $MSCOH$ stayed stable but relatively high for $K < K_{crit}$ and increases from K_{crit} onwards in the ideal case. When volume conduction was introduced, both curves were shifted toward higher $MSCOH$ values. Test statistic ks revealed that $MSCOH$ is highly affected by volume conduction: $ks = 0.26$ for $i_0 = 2$ and $ks = 0.41$ for $i_0 = 4$.

To summarize, our model simulations showed that the analyzed metrics are sensitive to increases in the coupling strength K. All three metrics responded to increases in the coupling strength for values of K higher than K_{crit}, but only AEC showed a good performance for K lower than K_{crit}. AEC and PLI are weakly influenced by the simulated volume conduction compared to $MSCOH$, although none of the analyzed metrics is immune to it. For these reasons, the subsequent analysis of the real EEG recordings was performed using only AEC, since this metric showed a better behavior for $K < K_{crit}$ compared to PLI despite the fact that AEC showed a slightly worse behavior in relation to volume conduction and sensitivity to coupling.

B. Real EEG recordings

Since results are frequency-dependent, AEC was computed for the six classical EEG-frequency bands: delta (δ, $1 - 4$ Hz), theta (θ, $4 - 8$ Hz), alpha (α, $8 - 13$ Hz), beta-1 (β_1, $13 - 19$ Hz), beta-2 (β_2, $19 - 30$ Hz), and gamma (γ, $30 - 70$ Hz). Connectivity patterns obtained for each frequency band are presented Fig. 2. Our AEC results showed that EEG activity in AD patients is characterized by widespread connectivity decreases in α and β_1 bands, and an overall increase of connectivity in δ band.

V. DISCUSSION

In the present study, we assessed the effect of volume conduction on the behavior of three connectivity metrics (AEC, PLI, and $MSCOH$) and their ability to reflect brain alterations suffered by AD patients with real EEG recordings.

For the first objective, we used the Kuramoto model with multiple oscillators centered at different mean frequencies and with frequency-dependent amplitudes, due to the fact that the combination of multiple oscillators may faithfully simulate the oscillatory nature of the EEG, and its behavior is very well studied [6]. Only Stam *et al.* [2] have previously employed the Kuramoto model to simulate the EEG activity. However, they modeled it using only one natural mean frequency at 10 Hz for all oscillators (corresponding to the predominant 'alpha band') with a constant amplitude for all oscillators. In our study, we present here an improved model with several oscillators. This has allowed us to create EEG-like signals that have enabled us to determine that AEC has the best performance detecting real changes in coupling.

Furthermore, a database of EEG recordings from 37 controls and 72 AD patients has been analyzed using AEC. Our results revealed that AD is characterized by a scattered increase in synchronization at δ band. In line with our results, an overall connectivity increase in δ band was previously reported for AD patients using $MSCOH$ [11]. On the other hand, a global decrease in synchronization at α and β_1 bands was found for AD patients [11]. Previous EEG studies have shown similar coupling evidences in AD through different connectivity metrics. For instance, Locatelli *et al.* [11] observed a decrease of the $MSCOH$ at α rhythms in the AD patients compared to the healthy controls. Similarly, Besthorn *et al.* [12] and Stam *et al.* [13] found a functional connectivity loss in AD, specifically in α and β bands using $MSCOH$ and synchronization likelihood, respectively.

Some limitations of our research work should be noted. Firstly, we propose a preliminary model of EEG volume conduction, taking into account only the effect of common sources by allowing more than a set of oscillators (centered at 1 Hz-separate frequencies) to contribute to each simulated EEG channel. It would be interesting to use a more realistic modeling of the EEG, taking into account the neurophysiological characteristics of the brain. Secondly, only three functional connectivity metrics have been analyzed in this

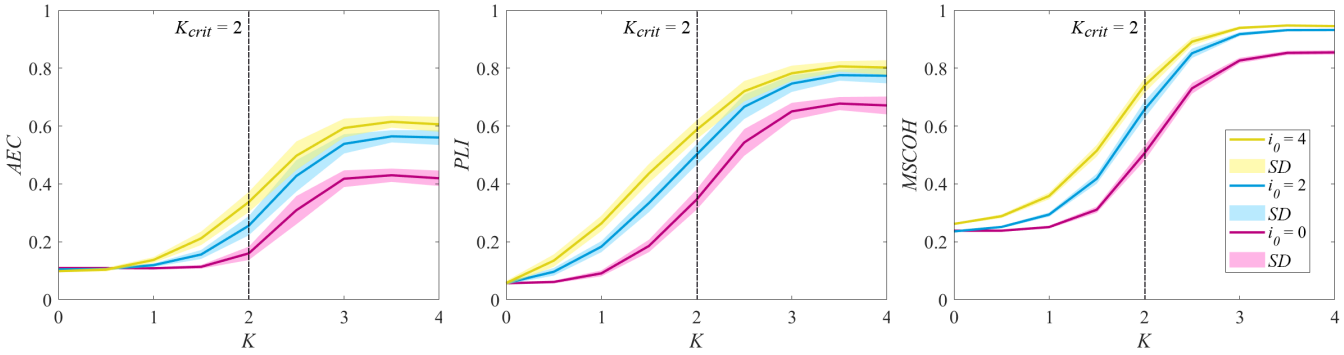

Fig. 1. AEC, PLI, and $MSCOH$ values as a function of global coupling intensity (K) for the different volume conduction contribution values (i_0). The solid lines indicate the average values and the shaded areas represent the standard deviation (SD) of 20 simulated epochs.

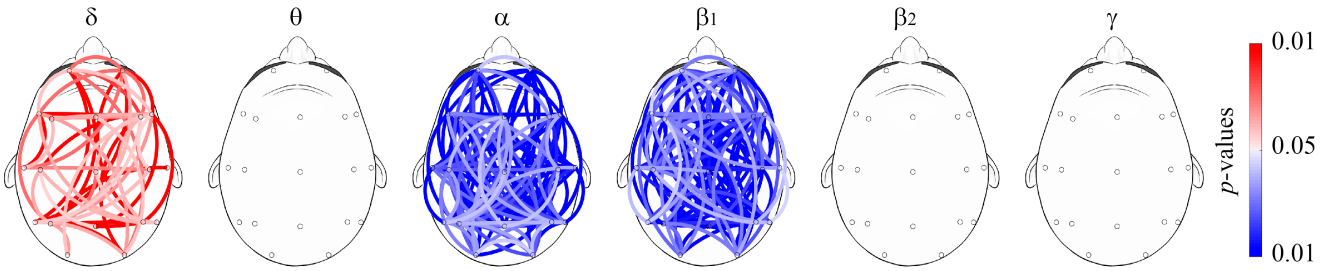

Fig. 2. AEC results for each classical EEG-frequency band. Connections between electrodes were only displayed when statistically significant within-group differences were obtained (Mann-Whitney U-test, FDR-corrected p-values < 0.05). Red color tones indicate statistically significant connectivity increases in AD patients in comparison with controls, whereas blue color tones denote significant decreases.

study, but other metrics could have a better behavior under volume conduction conditions, such as the imaginary part of coherence. Effective connectivity measures could also been explored, since they can have a different performance than functional ones, and provide additional information. Finally, only AD patients and healthy controls took part in this study. For future studies, it would be interesting to increase the number of healthy controls and to extend our analyses to prodromal AD stages, as mild cognitive impairment.

VI. CONCLUSIONS

Our study based on the Kuramoto models leads us to conclude that AEC have a slightly better performance detecting true changes in synchronization under volume conduction conditions compared to PLI, but $MSCOH$ is more affected by the influence of common sources. Furthermore, AEC revealed different connectivity patterns in EEG data for AD patients. Our results suggest that AD is associated with an overall coupling increase at δ band, and a decrease between different brain regions, mainly at α and β_1 frequency bands. These connectivity changes reflect the abnormalities in spontaneous EEG activity of AD patients, since AEC is a more reliable measure of true synchronization.

REFERENCES

[1] C. Babiloni, R. Lizio, N. Marzano, P. Capotosto, A. Soricelli, A. I. Triggiani, S. Cordone, L. Gesualdo, and C. Del Percio, "Brain neural synchronization and functional coupling in Alzheimer's disease as revealed by resting state EEG rhythms," *Int. J. Psychophysiol.*, vol. 103, pp. 88–102, 2016.

[2] C. J. Stam, G. Nolte, and A. Daffertshofer, "Phase lag index: Assessment of functional connectivity from multi channel EEG and MEG with diminished bias from common sources," *Hum. Brain Mapp.*, vol. 28, pp. 1178–1193, 2007.

[3] J. Jeong, "EEG dynamics in patients with Alzheimer's disease," *Clin. Neurophysiol.*, vol. 115, pp. 1490–1505, 2004.

[4] C. J. Stam and E. C. van Straaten, "The organization of physiological brain networks," *Clin. Neurophysiol.*, vol. 123, pp. 1067–1087, 2012.

[5] Y. Kuramoto, "Self-entrainment of a population of coupled non-linear oscillators," in *International Symposium on Mathematical Problems in Theoretical Physics*, Berlin, Heidelberg, 1975, vol. 39, pp. 420–422.

[6] S. H. Strogatz, "From Kuramoto to Crawford: Exploring the onset of synchronization in populations of coupled oscillators," *Physica D*, vol. 143, pp. 1–20, 2000.

[7] I. Z. Kiss, Y. Zhai, and J. L. Hudson, "Emerging coherence in a population of chemical oscillators," *Science*, vol. 296, pp. 1676–1678, 2002.

[8] M. J. Brookes, G. C. O'Neill, E. L. Hall, M. W. Woolrich, A. Baker, S. Palazzo Corner, S. E. Robson, P. G. Morris, and G. R. Barnes, "Measuring temporal, spectral and spatial changes in electrophysiological brain network connectivity," *NeuroImage*, vol. 91, pp. 282–299, 2014.

[9] G. C. O'Neill, P. Tewarie, D. Vidaurre, L. Liuzzi, M. W. Woolrich, and M. J. Brookes, "Dynamics of large-scale electrophysiological networks: A technical review," *NeuroImage*, vol. 180, p. 559–576, 2018.

[10] B. J. Roach and D. H. Mathalon, "Event-related EEG time-frequency analysis: An overview of measures and an analysis of early gamma band phase locking in schizophrenia," *Schizophr. Bull.*, vol. 34, pp. 907–926, 2008.

[11] T. Locatelli, M. Cursi, D. Liberati, M. Franceschi, and G. Comi, "EEG coherence in Alzheimer's disease," *Electroencephalogr. Clin Neurophysiol.*, vol. 106, pp. 229–237, 1998.

[12] C. Besthorn, H. Förstl, C. Geiger-Kabisch, H. Sattel, T. Gasser, and U. Schreiter-Gasser, "EEG coherence in Alzheimer disease," *Electroencephalogr. Clin. Neurophysiol.*, vol. 90, pp. 242–245, 1994.

[13] C. J. Stam, Y. Van Der Made, Y. A. L. Pijnenburg, and P. Scheltens, "EEG synchronization in mild cognitive impairment and Alzheimer's disease," *Acta Neurol. Scand.*, vol. 108, no. 2, pp. 90–96, 2003.